Spectrochimica Acta Part A: Molecular and Biomolecular Spectroscopy 200 (2018) 330–338

Contents lists available at ScienceDirect

Spectrochimica Acta Part A: Molecular and Biomolecular Spectroscopy

journal homepage: www.elsevier.com/locate/saa

An aptamer-based fluorescence bio-sensor for chiral recognition of arginine enantiomers

Haiyan Yuan [a,b], Yunmei Huang [a,b], Jidong Yang [a,b,*], Yuan Guo [a,b], Xiaoqing Zeng [a,b], Shang Zhou [c], Jiawei Cheng [a,b], Yuhui Zhang [a,b]

[a] Key Laboratory of Water Environment Evolution and Pollution Control in Three Gorges Reservoir, Chongqing Three Gorges University, PR China
[b] School of Environment and Chemical Engineering, Chongqing Three Gorges University, Chongqing 404100, PR China
[c] College of Chemistry and Chemical Engineering, Yangtze Normal University, Chongqing 408100, PR China

ARTICLE INFO

Article history:
Received 21 March 2018
Received in revised form 12 April 2018
Accepted 17 April 2018
Available online 21 April 2018

Keywords:
Aptamer
Bio-sensor
Chiral recognition
Arg enantiomers
Logic gate

ABSTRACT

In this study, a novel aptamer - based fluorescence bio-sensor (aptamer-AuNps) was developed for chiral recognition of arginine (Arg) enantiomers based on aptamer and gold nanoparticles (AuNps). Carboxyfluorescein (FAM) labeled aptamers (Apt) were absorbed on AuNps and their fluorescence intensity could be significantly quenched by AuNps based on fluorescence resonance energy transfer (FRET). Once D-Arg or L-Arg were added into the above solution, the aptamer specifically bind to Arg enantiomers and released from AuNps, so the fluorescence intensity of D-Arg system and L-Arg system were all enhanced. The affinity of Apt to L-Arg is tighter to D-Arg, so the enhanced fluorescence signals of L-Arg system was stronger than D-Arg system. What's more, the enhanced fluorescence were directly proportional to the concentration of D-Arg and L-Arg ranging from 0–300 nM and 0–400 nM with related coefficients of 0.9939 and 0.9952, respectively. Furthermore, the method was successfully applied to detection L-Arg in human urine samples with satisfactory results. Eventually, a simple "OR" logic gate with D-Arg & L-Arg as inputs and AuNps aggregation state as outputs was fabricated, which can help us understand the chiral recognition process deeply.

1. Introduction

Chiral recognition of biomolecules and drugs have attracted tremendous attentions. It's well known that most chiral drugs existed in the form of racemic mixture; however, because of the specific recognition and toxicological activities, sometimes only a single enantiomer is non-poisonous and medicable for human. For example, R-thalidomide has the medicable function while S-thalidomide has the toxic properties [1]. Most natural amino acids exist in the bio-organism are L-amino acids and most carbohydrates are D-carbohydrates, that is to say only L-amino acids and D-carbohydrates are nutritious to human body. Consequently, simultaneous determination of chiral enantiomers is pretty vital in clinical research and pharmacy industry.

Arg is a kind of chiral amino acid, which existed in the form of D-Arg or L-Arg. The ball-and-stick model and subtle structure difference of D/L-Arg were shown in Fig. 1. L-Arg was involved in the ornithine cycle in human body, played a role in turning ammonia into non-toxic urea and reducing the concentration of blood ammonia [2]. For infants, L-Arg counts for much during their growing process because infants are unable to synthesize or create internally, but for most adults, L-Arg is not essential because their body can produce enough. Consequently, L-Arg is defined as essential or nonessential amino acid depending on the healthy conditions of people [3]. A precious research claimed that Arg breakdown will highlight the early stages of dementia disease in mice. Arg is also supplied to correct the acid and alkali balances in hepatic encephalopathy because of its rich hydrogen ions. If infants are severe deficiency of Arg, they will be troubled by cardiovascular, pulmonary, neurological and intestinal dysfunction [4,5]. Thus, establish a simple, rapid, low cost and highly selective method for the detection of Arg enantiomers is significant important. Up to now, many methods have been applied to detection chiral enantiomers, such as high-performance liquid chromatography (HPLC) [6–8], gas/liquid chromatography-mass spectrometry (GC/LC-MS) [9,10], fluorescence spectrometry [11,12], electrochemistry [13,14], and immunoassays [15]. Among these methods, HPLC, electrochemistry and GC/LC-MS need complicated pretreatment and require expensive chiral columns. Therefore, sensitive and simple methods have been strongly required.

Since discovered in 1990 [16], aptamers have attracted much attention. Aptamer is a new type of single-strand DNA (ssDNA) or RNA oligonucleotides, selected in vitro through Systematic Evolution of Ligands by Exponential enrichment (SELEX) [17,18]. In addition, aptamers have high selectivity which derived from their specific hairpin structure, therefore, aptamer can distinguish between similar compounds with

* Corresponding author.
E-mail address: flyjd6400@sina.com. (J. Yang).

https://doi.org/10.1016/j.saa.2018.04.038
1386-1425/

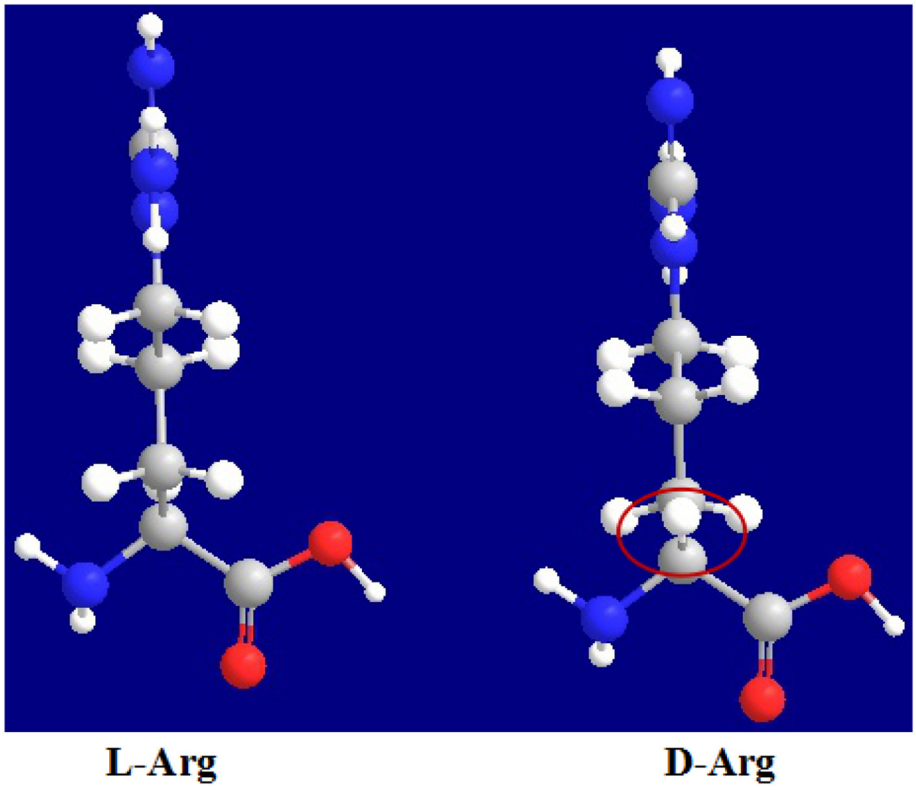

Fig. 1. The ball-and-stick model of Arg.

only subtle structure difference [19,20]. For example, Michael Famulok et al. [21] reported that the RNA aptamer had an affinity to L-Arg and bound 12,000 bold tighter than to its enantiomer, D-Arg. The recognizing process of aptamer is similar to the antibodies but in terms of high stability, low-cost, easy synthesis and flexible chemical labeling, aptamers are better than antibodies. Aptamer are utilized as various sensors, according to the differences of signals obtained, aptasensors are divided into eletrochemical [22,23] optical [24] and mass-sensitive [25]. For example, Citartan Marimuthu and their workers used electrochemical aptasensor for chiral recognition of S-naproxen from R-naproxen. Yuan Huo, Xin Lv had established fluorescence and colorimetry methods based on optical aptasensors [26,27]. Zhi-Qi Zhang et al. [28], Shulin Yang et al. [29] developed a DNA aptasensor for the colorimetric detection of adenosine triphosphate, arginine vasopressin and omethoate, respectively. Shuhao Wang et al. [30] reported a florescence signals off-on aptasensor for fluorescent detection of ochratoxin A based on the quenching effect of gold nanoparticles and showed a linear range from 25 nM to 300 nM. Erkang Wang [31] and their workers developed a fluorescent indicator for D-arginine vasopressin detection. In 2005, Arg - specific aptamer was first screened out through SELEX [32]. To the best of our knowledge, there almost no research reported about simultaneous detection of chiral Arg enantiomers based on aptamer-AuNps biosensor.

Gold nanoparticles (AuNps) were widely used in chemical and biological detection because of their outstanding advantages, including extremely high extinction coefficients, strong size, distance-dependent

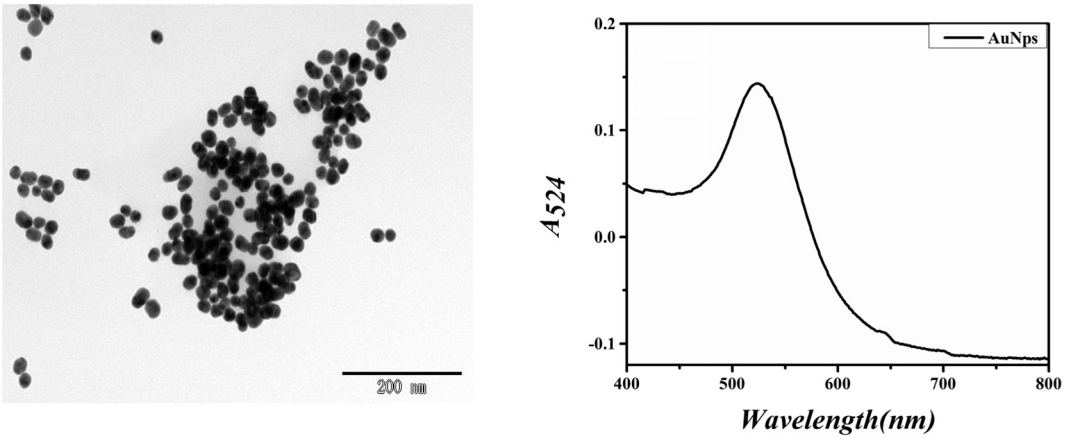

Fig. 2. (A) The TEM image and (B) UV–vis absorption spectra of AuNps in 50 μL Tris-HCl buffer solution at pH = 7.2.

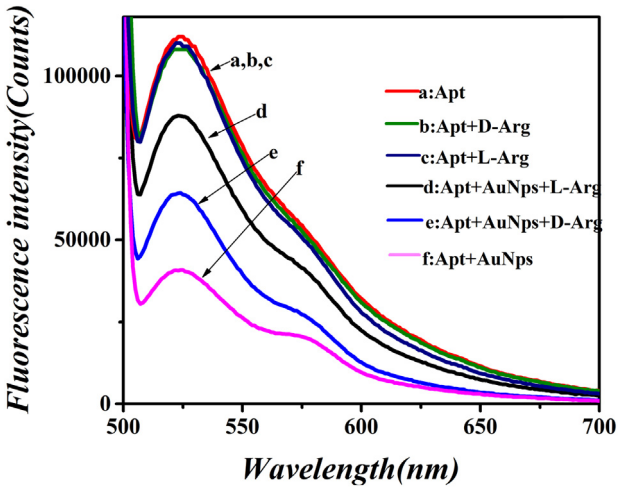

Fig. 3. Fluorescence emission spectra of Apt (a) Apt + D-Arg (b) Apt + L-Arg (c) Apt + AuNps + L-Arg (d) Apt + AuNps + D-Arg (e) Apt + AuNps (f) in 50 μL Tris-HCl buffer solution at pH = 7.2. AuNps: 10 nM·L^{-1}, Apt: 60 nM·L^{-1}, D/L-Arg: 120 nM·L^{-1}.

optical properties and their high quenching efficiency towards various fluorophores [33]. The fluorescence quenching principle of AuNps generally contains fluorescence resonance energy transfer (FRET) or inner filter effect (IFE) [34,35]. Compared with traditional modified AuNps, the citrate-protected AuNps are more stable and maintain disperse. In this study, a fluorescence method with aptamer-AuNps biosensor was developed to discriminate Arg enantiomers. In the absence of Arg enantiomers, carboxyfluorescein (FAM) modified aptamer got absorbed onto the surface of AuNps and the fluorescence can be effectively quenched by AuNps. While after adding Arg enantiomers (D/L-Arg) into the aptamer + AuNps system, the specific recognition between aptamer and D/L-Arg resulting aptamer bind to D/L-Arg and released the AuNps into solution, fluorescence intensity of the D/L-Arg system all increased. Interestingly, the recovered fluorescence intensity of Apt + AuNps + L-Arg system was stronger than Apt + AuNps + D-Arg system. Therefore, an aptamer + AuNps biosensor was established for simultaneous determine Arg enantiomers. Eventually, this fluorescence analytical method was applied in real sample analysis and satisfactory results were obtained. A logic gate was also established to help us understand the chiral recognition process better.

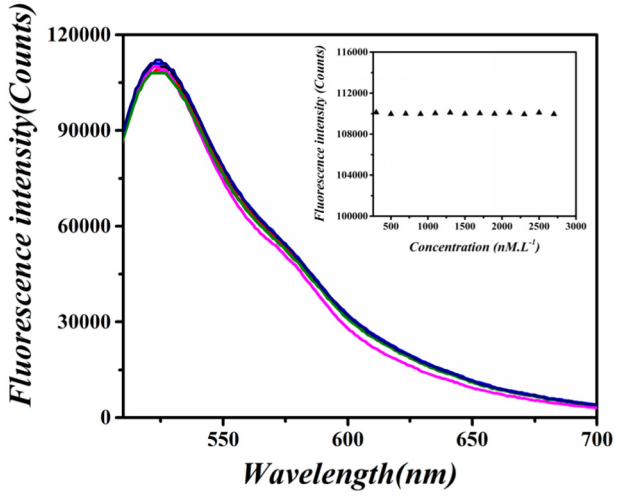

Fig. 4. Fluorescence spectra of Apt in the presence of L-Arg in 50 μL Tris-HCl buffer solution at pH = 7.2; the inset shows the linear of the quenched fluorescence intensity of Apt against the concentration of L-Arg. (Apt: 60 nM·L^{-1}; L-Arg: 0.0, 300, 500, 700, 900, 1100, 1300, 1500, 1700, 1900, 2100, 2300, 2500, 2700 nM·L^{-1}).

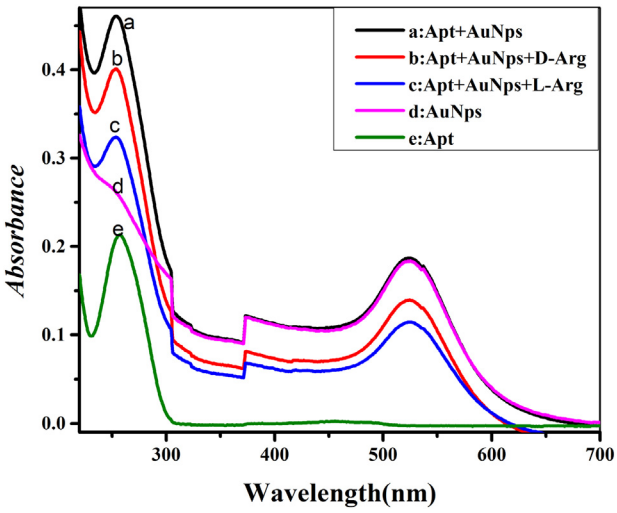

Fig. 5. UV–vis spectra of AuNPs in different systems with 50 uLTris-HCl buffer solution. a: AuNps + Apt. b: AuNPs + Apt + D-Arg. c: AuNPs + Apt + L-Arg. d: AuNps. e: Apt. Experiment conditions: AuNps: 10 nM·L^{-1}, Apt: 60 nM·L^{-1}, D/L-Arg: 120 nM·L^{-1}, pH = 7.2.

2. Experimental

2.1. Materials

Aptamer used in this work were synthesized and purified with ULTRPAGE by Sangon Biotechnology Co., Ltd. (Shanghai, China, http://www.sangon. com). The sequence of carboxyfluorescein (FAM) labeled aptamer from 5′ to 3′ was 5′-FAM-ATA CCA GCT TAT TCA ATT TGA GGC GGG TGG GTG GGT TGA ATA CGC TGA TTA CCC CAT CGG AGA ACG TTA AGG CGC TTC AGA TAG TAA GTG CAA TCT-3′ (FAM-Apt) and the secondary structure of the Apt were shown in Fig. S1, which was determined by Reinemann et al [36]. The stock solution was prepared by dissolving the lyophilized DNA powder in distilled water and its concentration was 0.5 μM then stored at 4 °C before using. Chloroauric acid ($HAuCl_4$), sodium citrate, arginine enantiomers (D/L-Arg) were purchased from Shanghai Chemical Reagent Company (Shanghai, China). Other chemical reagents, including sodium chloride, histidine enantiomers, cysteine enantiomers, phenylalanine enantiomers, tyrosine enantiomers and all chemicals used in this work were of analytical grade which can be used directly without further purification. Ultrapure water was obtained from a Millipore water purification system (≥18 MΩ, Milli-Q Millipore) and used for all experiments. The urine samples were collected from healthy volunteers among the co-authors of the School of environment and chemical engineering, *Chongqing Three Gorges University* (*CQTGU*), China. The utilization of human urine was approved by the *Chongqing Three Gorges University's Institutional Review Board.*

2.2. Apparatus

FS5 fluorescence spectrometer (Edinburgh Instruments, Edinburgh, Scotland) with excitation and emission slit width of 14 nm was applied to record fluorescence (FL) spectra. The excitation wavelength was 485 nm and the emission spectra were recorded from 510 nm to 650 nm. And the optical path of a quartz fluorescence cell was 1.0 cm. The absorption spectra were recorded on Shimadzu UV-2700 spectrophotometer (Shimadzu Corporation, Kyoto, Japan). Transmission electron microscopy (TEM) images of AuNps in different system were obtained from JEM-1200 EX transmission electron microscopy (Electronics Corporation, Japan). pH values were measured by pHS-3C-02 m (Shanghai San-Xin Instrumentation Inc., Shanghai, China).

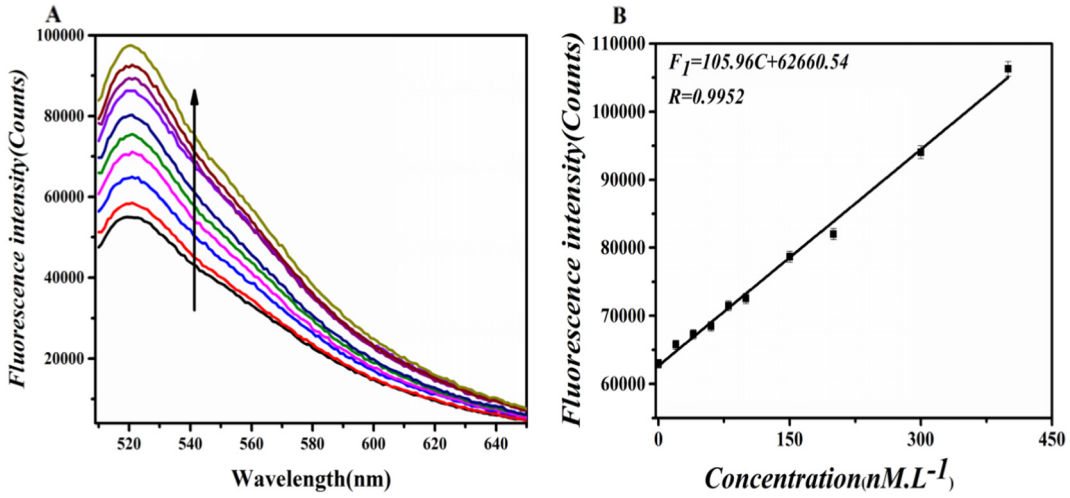

Fig. 6. A. Fluorescence spectra of aptamer with the addition of 10 nM·L^{-1} of AuNps recover due to introducing L-Arg in the concentration range of 0 to 400 nM·L^{-1}. B. The liner calibration plot of the fluorescence intensity against the concentration of L-Arg. Concentration of aptamer: 60 nM·L^{-1}; Concentration of AuNps: 10 nM·L^{-1}. Concentration of L-Arg: 0, 20, 40, 60, 80, 100, 150, 200, 300, 400 nM·L^{-1}, respectively. Tris-HCl buffer solution, 50 μL, pH = 7.2.

2.3. Synthesis of the Citrate-protected AuNps

The AuNps were synthesized according to the method reported before [37]. Briefly, 50 mL of 0.01(w/v) $HAuCl_4$ solution was heated to boiled under continuous stirring, and then 750 μL, 1% sodium citrate ($Na_3C_6H_5O_7.2H_2O$) was quickly added to the above solution. The color of the solution changed from blue to red-violet within 95 s. Further heating and stirring the boiled solution for an additional 10 min, then remove the heating source when the solution turned deep red, continuously stirred for another 15 min. A transparent deep-red solution of AuNps was obtained without further purification. The solution was cooled to room temperature and stored at 4 °C before using and its morphology images was characterized by transmission electron microscopy (TEM). The dispersed state of AuNps can general maintain fifteen days. The concentration of AuNps was calculated to be about 15 nM·L^{-1} using Lambert Beer's law with an extinction coefficient of 2.78 × 10^8 M^{-1}·cm^{-1} at ~520 nm [38].

2.4. Chiral Recognition of Arg Enantiomers Based on Aptamer-AuNps Biosensor

Typically, all glasswares used in the following procedure were soaked in aqua regia (HNO_3/HCl = 1:3, v/v) about 5 h, then thoroughly cleaned in water and over-dried prior to use. Firstly, 60 μL 0.5 μM·L^{-1} aptamer, 50 μL 15 nM·L^{-1}AuNps, 50 μL Tris - HCl buffer solution (pH 7.2) were mixed and incubated for 40 min in order that they can interact with each other sufficiently. Secondly, sample solutions contain different concentration of D-Arg and L-Arg solution were respectively added into the above mixtures, and then incubated for another 45 min at room temperature. Eventually, the mixed solution was diluted with deionized water to 500 μL. The fluorescence intensity was recorded by a FS5 fluorescence spectrometer using excitation wavelength of 485 nm. And the fluorescence intensity of the maximum emission peak (λ = 524) was used for quantitative detection of D-Arg and L-Arg.

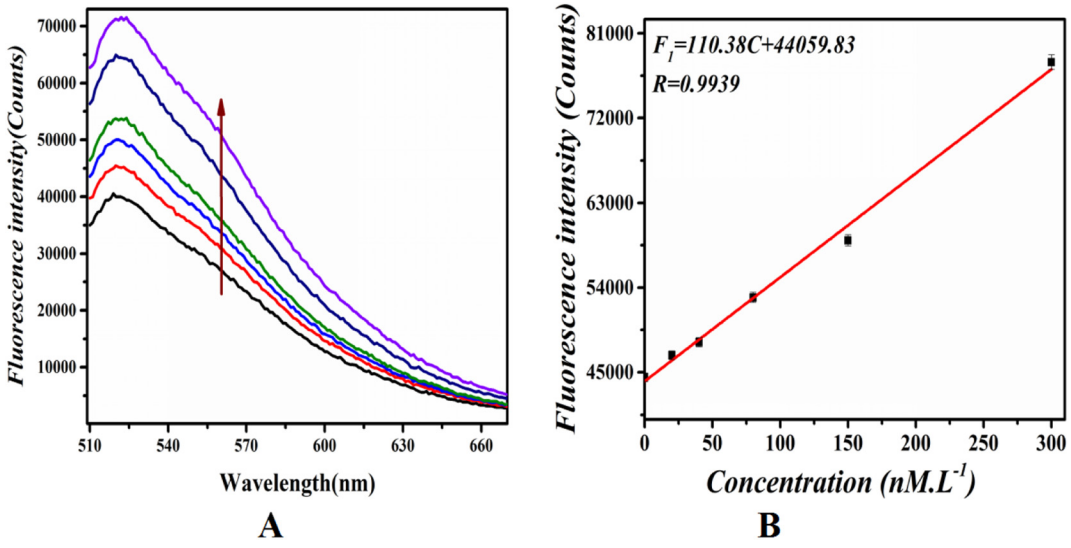

Fig. 7. A. Fluorescence spectra of aptamer with the addition of 10 nM·L^{-1} of AuNps recover due to introducing D-Arg in the concentration range of 0 to 300 nM·L^{-1}. B. The liner calibration plot of the fluorescence intensity against the concentration of D-Arg. Concentration of aptamer: 60 nM·L^{-1}; Concentration of AuNps: 10 nM·L^{-1}. Concentration of D-Arg: 0, 20, 40, 80, 150, 300 nM·L^{-1}, respectively. Tris-HCl buffer solution, 50 μL, pH = 7.2.

Table 1
Comparison of various methods reported before for Arg sensing.

Methods	Range	LOD	Ref.
Electrochemical	0–8.61 × 10^{-7} M	1.6 × 10^{-12} M	3
Azo nano-materials biosensor	5 × 10^{-6}–5 × 10^{-5} M	8 × 10^{-7} M	45
Nanoparticles/Cds quantum dots	4 × 10^{-8}–1.23 × 10^{-6} M	1.37 × 10^{-8} M	46
Carbon nano-dots	0–10^{-4} M	2.6 × 10^{-7} M	47
Conductometric biosensor	1.0 × 10^{-5}–1.0 × 10^{-3} M	1.0 × 10^{-5} M	48
Carbon fiber cylinder	5 × 10^{-4}–5 × 10^{-3} M	1.0 × 10^{-5} M	49
DNA aptamer	2.5 × 10^{-8}–4 × 10^{-7} M	1.8 × 10^{-9} M	This work

2.5. Application in Urine Samples

In order to investigate the feasibility of this method for practical analysis, urine samples with different concentration of L-Arg were performed. The procedure for L-Arg determination (just L-Arg exist in human body so we only tested L-Arg) in urine samples was in accordance with the above statement in part 2.4. Urine samples were centrifuged at 13,000 rpm for 15 min to remove particulates and diluted 1000-fold to avoid interference from the urine sample. Each sample was tested five times and recoveries, relative standard deviations of the samples were investigated.

3. Results and Discussion

3.1. Characterization of AuNps

As shown in Fig. 2(A), the morphology of the as-prepared citrate-protected AuNps was investigated by TEM. It is quite evident that these nanoparticles are close to spherical and with an average diameter of 12 nm. Besides, these spherical nanoparticles are nearly dispersive. Previous literature had reported the dispersed state derive from the negative capping agents (citrateion) electrostatic repulsion against van der Waals attraction between AuNps [39]. The UV–vis absorption spectrum of the as-prepared citrate - wrapped AuNps was also tested shown in Fig. 2(B), the UV–vis absorption spectrum shows a strong absorption in the ultraviolet region, and the characteristic surface plasma absorption peak is located at 524 nm.

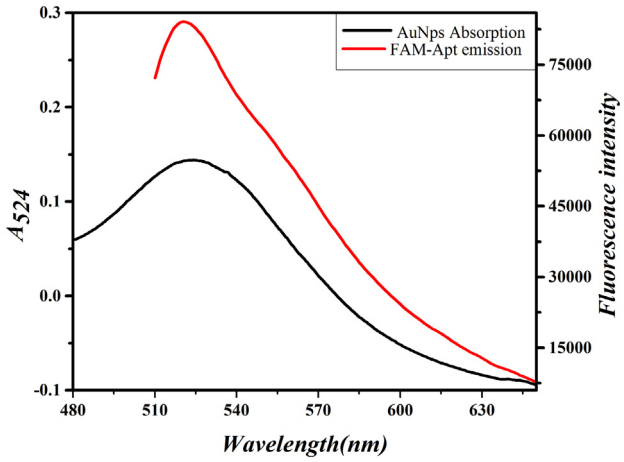

Fig. 8. Overlap between fluorescence emission of FAM-Apt and the absorbance spectrum of AuNPs in 50 μL Tris-HCl buffer solution at pH = 7.2; Concentration of FAM-Apt: 60 nM·L^{-1}, concentration of AuNps: 10 nM·L^{-1}.

3.2. Chiral Recognition of Arg Enantiomers Based on Aptamer-AuNps Biosensor

3.2.1. Fluorescence Spectra for Chiral Recognition of Arg Enantiomers

The fluorescence spectra of aptamer in different experiments system were investigated. As shown in Fig. 3, the fluorescence intensity of FAM-aptamer (Apt) at 524 nm (excitation wavelength is 485 nm) was very strong (Fig. 3, curve a) and close to unchanged after added D/L-Arg (Fig. 3, curve b, c) into Apt solution. Indicating D/L-Arg can't quench the fluorescence of Apt directly. However, when added AuNps to the aptamer system, the work got interesting. First, the fluorescence intensity of Apt solution was dramatically quenched by AuNps (Fig. 3, curve f). Then, respectively added D/L-Arg into the above mixtures, there appear different degree of fluorescence enhancement and the L-Arg system enhanced stronger than D-Arg system (Fig. 3, curve d, e). In order to further confirm whether Arg enantiomers can directly quench the fluorescence of Apt, the fluorescence spectra of aptamer after adding a series concentration of D/L-Arg were investigated. As shown in Fig. 4, the concentration of L-Arg was enlarged to 10 times while the fluorescence intensity remained almost unchanging. Correspondingly, the fluorescence intensity of Apt with various concentration of D-Arg remained unchanging, too (data not shown). That is to say neither D-

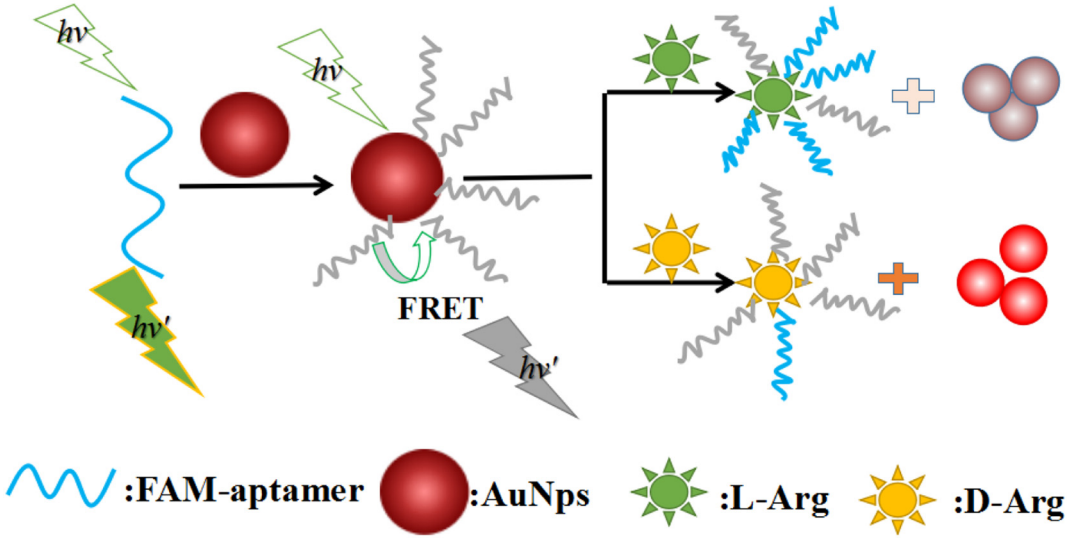

Scheme 1. Schematic illustration of the fluorescence method for D,L-Arg detection based on the aptamer-AuNps fluorescence chiral bio-sensor.

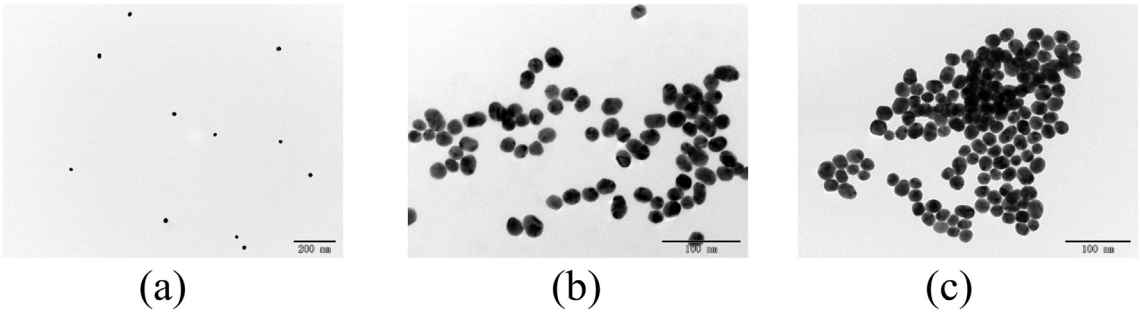

Fig. 9. TEM images of AuNps in different system in 50 μL Tris-HCl buffer solution at pH = 7.2. (a) AuNps + aptamer (b) AuNps + aptamer + D-Arg (c) AuNps + aptamer + L-Arg. Concentration of FAM-Apt: 60 nM·L^{-1}, concentration of AuNps: 10 nM·L^{-1}. Concentration of D/L-Arg: 120 nM·L^{-1}.

Arg nor L-Arg can quench the fluorescence intensity of Apt in the absence of AuNps. In other words, only when aptamer and AuNps concurrent existence can realize chiral recognition of arginine enantiomers and so in this work we defined Apt-AuNps complexes as the chiral bio-sensor.

3.2.2. UV–vis Absorption Spectra for Chiral Recognition of Arg Enantiomers

The absorbance spectra of AuNps in different experiment system were also investigated. As shown in Fig. 5, there is a maximum absorption peak at 524 nm for the AuNps (Fig. 5, curve d). After added Apt, the characteristic absorption peak of Apt appeared at about 252 nm and the absorbance intensity increased greatly (Fig. 5, curve a), which indicated AuNps have interacted with Apt. Continuously introducing appropriate amount of D-Arg or L-Arg into the above system, both the absorbance of D/L-Arg system decreased and L-Arg decreased heavily than D-Arg (Fig. 5, curve b, c). The results demonstrate the affinity of aptamer to D-Arg and to L-Arg are different.

3.3. Determination of D/L-Arg

3.3.1. Determination of L-Arg

Based on the primary experiment phenomenon we obtained, a new fluorescence method based on aptamer-AuNps bio-sensor was proposed for detection Arg enantiomers. As shown in Fig. 6A, under optimum conditions, the fluorescence intensity of the sensor enhanced with the concentration of L-Arg increasing. As demonstrated in Fig. 6B, a linear calibration plot of the fluorescence intensity (F1) against the concentration of L-Arg was observed in the range of 0–400 nM·L^{-1} with a correlation coefficient of 0.9952 and a linear regression equation of F1 = 105.96C + 62,660.54 (where C is the concentration of L-Arg in nM·L^{-1}). The limit of detection for L-Arg was determined to be 1.9 nM, which was determined by 3σ/S, σ is the standard deviation of instrument and S is the slope the linear calibration plot.

3.3.2. Determination of D-Arg

Under optimum conditions, the fluorescence spectra of aptamer-AuNps sensor with different concentration of D-Arg were also tested. As shown in Fig. 7A, the results showed that the enhanced fluorescence intensity were directly proportional to the concentration of D-Arg in a certain range of 0–300 nM·L^{-1}. In Fig. 7B, it exhibited a good linear relationship in the range of 0–300 nM·L^{-1}. The linear regression equation was determined to be Y = 110.38C + 44,059.83 (where C is the concentration of D-Arg in nM·L^{-1}) and the correlation coefficient is 0.9939.

It is worth mentioning that L-Arg exhibited better linear relation on fluorescence intensity than that of D-Arg in the presence AuNps, which indicated that Apt + AuNps bio-sensor can really achieve high enantioselective recognition of Arg enantiomers. In addition, compared with other methods reported before (Table 1), this method is comparable and more sensitive and has relatively wider linear range.

3.4. Principle of Chiral Recognition of Arg Enantiomers With Aptamer-AuNps Sensor

Aptamer possess outstanding bio-compatibility and specific recognition ability, so they have been widely applied in detection of proteins,

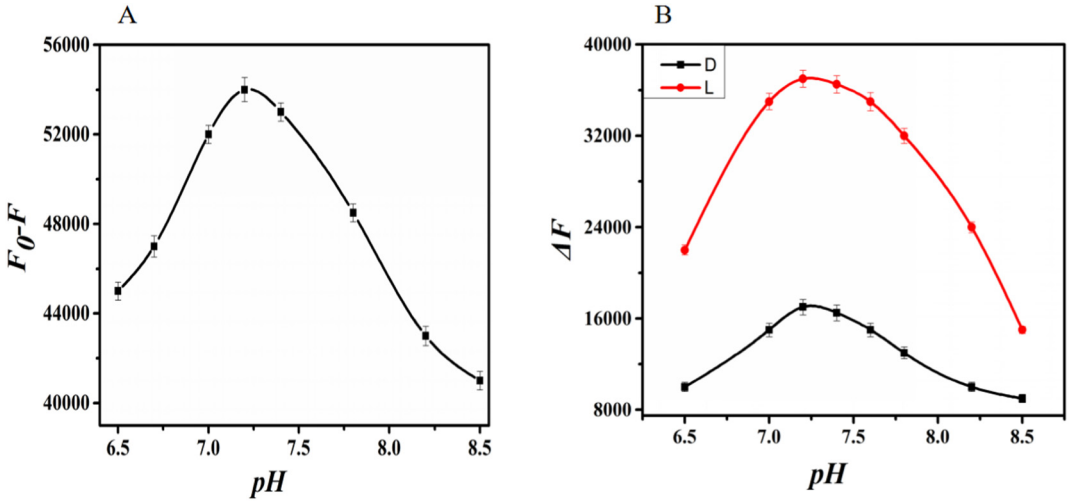

Fig. 10. A. Effect of acidity on the decrease of fluorescence intensity of FAM-aptamer after the addition of AuNps in the Tris-HCl buffer solution (FAM-aptamer:60 nM·L^{-1}, AuNps:10 nM·L^{-1}); B. Effect of acidity on the recovery of fluorescence intensity of FAM-aptamer and AuNps system after the addition of D/L-Arg in the Tris-HCl buffer solution (FAM-aptamer:60 nM·L^{-1}, AuNps: 10 nM·L^{-1}; D/L-Arg: 120 nM·L^{-1}).

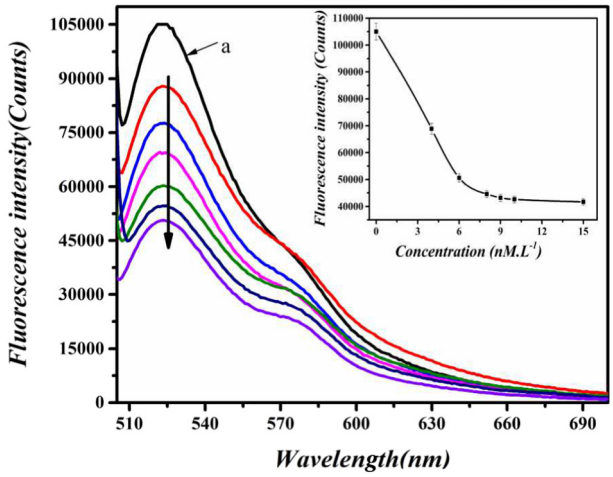

Fig. 11. Effects of concentration of AuNps on fluorescence intensity (curve a: the fluorescence spectra of Apt). Experimental conditions: FAM-Apt: 60 nM·L^{-1}; 50 μL Tris-HCl buffer solution, pH = 7.2.

DNA and small molecules. Moreover, DNA aptamer can uncoil sufficiently to expose their bases, and can be adsorbed on the bare colloidal AuNps [40] rapidly. While gold nanoparticles (AuNps) have extremely high extinction coefficients, so they have high quenching efficiency towards various fluorophores [41]. The mechanism was depicted in Scheme 1. FAM-aptamer has high fluorescence signals in the absence of AuNps. However, when the FAM-aptamer solution was introduced AuNps, because the electrostatic interactions between FAM-aptamer and AuNps, aptamer was absorbed on the negatively charged AuNps and the fluorescence of aptamer was effectively quenched via the fluorescence resonance energy transfer (FRET) from FAM-Apt to AuNps. Following, respectively adding Arg enantiomers into the sensing system, FAM-aptamer specifically combined with its targets (D, L-Arg) and released from AuNps, resulting in the fluorescence recovery and the aggregation of AuNps. While the affinity of aptamer to L-Arg is tighter than to D-Arg, so the recovered fluorescence intensity of L-Arg is stronger than its enantiomer, D-Arg.

In order to further confirm there really exist fluorescence resonance energy transfer (FRET) between aptamer and AuNps, the absorption spectrum of AuNps and the fluorescence emission spectrum of FAM - Apt were investigated respectively. As illustrated in Fig. 8, AuNps showed a well-defined absorption peak at 524 nm, this wavelength was almost the same as that of emission wavelength of FAM-Apt, and

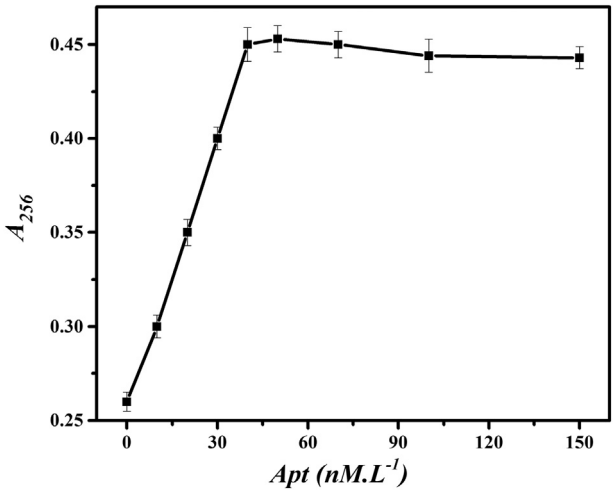

Fig. 12. Effects of different concentration of aptamer on A_{256} of AuNps. Experimental conditions: AuNps 10 nM·L^{-1}; 50 μL Tris-HCl buffer solution, pH = 7.2.

the absorption spectrum of AuNps overlapped partially with the fluorescence emission spectrum of FAM - Apt, indicating that FRET was really between them. So the fluorescence intensity of FAM-Apt was significantly quenched by AuNps.

Some researches have demonstrate that the fluorescence intensity is related to the aggregation degree, so transmission electron microscopy (TEM) images of AuNps in different system were also tested to observe the aggregation or dispersion state. Fig. 9 shows that in the presence of aptamer, AuNps remained well dispersed (Fig. 9(a)). However, when added a certain D-Arg into the above system, AuNps aggregated into minor cluster, indicated small amount of aptamer were bind to D-Arg (Fig. 9(b)). In contrast, when adding L-Arg into the aptamer + AuNps system (Fig. 9(c)), the majority aptamer combined with L-Arg, so AuNps aggregated into larger clusters. The results from TEM images were well demonstrate the affinity of aptamer to D-Arg and to L-Arg were different, so the enhanced fluorescence intensity of L-Arg system and D-Arg system were different.

3.5. Optimization of Detection Conditions

Appropriate experiment parameters are very important because these factors can affect the results of the entire experiment. To obtain accurate and satisfactory results, different experimental conditions for chiral recognition of Arg enantiomers were optimized, such as the concentration of FAM - Apt, concentration of AuNps, reaction time, and pH value.

3.5.1. Effect of pH Value

The pH of the solution not only strongly affected the fluorescence quenching of AuNps towards the FAM-aptamer but also effected the fluorescence restoration ability of Arg enantiomers. In this work, we used Tris-HCl as the buffer solution. As shown in Fig. 10, the influence of pH on the fluorescence intensity of FAM-aptamer + AuNps system and FAM-aptamer + AuNps + Arg enantiomers has been investigated, respectively. From Fig. 10A we know the pH of the solution influenced the fluorescence quenching ability of AuNps to FAM-aptamer significantly, the maximum value of F0-F was obtained when the pH value was 7.2 (F0 and F were the fluorescence intensities of the aqueous FAM-aptamer without and with a given concentration of AuNps). Therefore, the optimal pH of FAM-aptamer + AuNps system was 7.2. More importantly, we must seek out the optimum pH in the recovery system. In Fig. 10B, we can see that the maximum fluorescence recovery (ΔF, ΔF = F1 − F, F and F1 were the fluorescence intensities of the aqueous FAM-aptamer + AuNps system with and without a given concentration of Arg enantiomers) of FAM-aptamer + AuNps system after the addition of Arg enantiomers was obtained at pH 7.2, which fitted well with the optimum pH (7.2) of FAM-aptamer + AuNps system. Hence, we chose pH = 7.2 as the optimized pH value in this work.

3.5.2. Effect of the Concentration of AuNps

The fluorescence intensity and the analytical performance of whole sensing system were significantly influenced by the concentration of AuNps. As depicted in Fig. 11, the fluorescence intensity of aptamer was markedly decreased with increasing the concentration of AuNps to 10 nM. However, when the concentration of AuNps was higher than 10 nM·L^{-1}, the fluorescence intensity was almost unchanged. Indicating that AuNps were all wrapped by aptamer and the fluorescence quenching efficiency was sufficient. So the optimized concentration of AuNPs was 10 nM·L^{-1}.

3.5.3. Effect of the Concentration of FAM-aptamer

The concentration of aptamer was another vital factor, as illustrated in Fig. 12, A_{256} is the absorbance of AuNps at 256 nm, when the concentration of aptamer higher than 60 nM, the excessive aptamer lead to requirement of too much Arg enantiomers to release the aptamer from AuNps and would low sensitivity about the assay. While when the

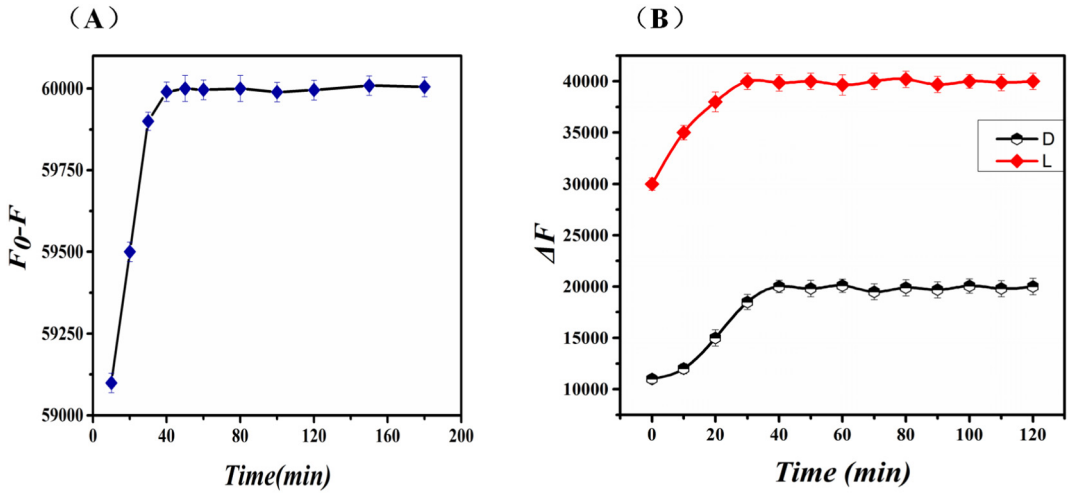

Fig. 13. (A) Effect of reaction time on the decrease of fluorescence intensity of FAM-aptamer after the addition of AuNps in the Tris-HCl buffer solution (FAM-aptamer:60 nM·L^{-1}, AuNps: 15 0 M·L^{-1}); (B) Effect of reaction time on the recovery of fluorescence intensity of FAM-aptamer and AuNpS system after the addition of D/L-Arg in the Tris-HCl buffer solution (FAM-aptamer: 60 nM·L^{-1}, AuNps: 10 nM·L^{-1}; D/L-Arg: 120 nM·L^{-1}).

concentration of aptamer was <60 nM, A_{256} increased apparently, signifying that AuNps were not protected by aptamer and aggregated. Thus, the optimized aptamer concentration was 60 nM in the reaction system.

3.5.4. Effect of Reaction Time

The influence of reaction time on the fluorescence intensity of FAM-aptamer + AuNps system and FAM-aptamer + AuNps + Arg enantiomers system were investigated eventually. In Fig. 13(A), the results revealed that the maximum value of F0-F (F0 and F were the fluorescence intensities of the aqueous FAM-aptamer without and with a given concentration of AuNps) maintained almost unchanged after 40 min, indicating that FAM-aptamer were completely adsorbed on the surface of AuNps within 40 min. Thus, 40 min was chosen for the fluorescence quenching experiments. The biding time of FAM-aptamer and Arg enantiomers were also optimized, in Fig. 13(B), the experiments results showed when the reaction time reach to 45 min, there occurred the maximum fluorescence recovery (ΔF=F1 − F, F and F1 were the fluorescence intensities of the aqueous FAM-aptamer + AuNps system with and without a given concentration of Arg enantiomers) and the fluorescence intensity of the ternary system was stable within 2 h. Therefore, 40 min was chosen for the fluorescence recover experiments.

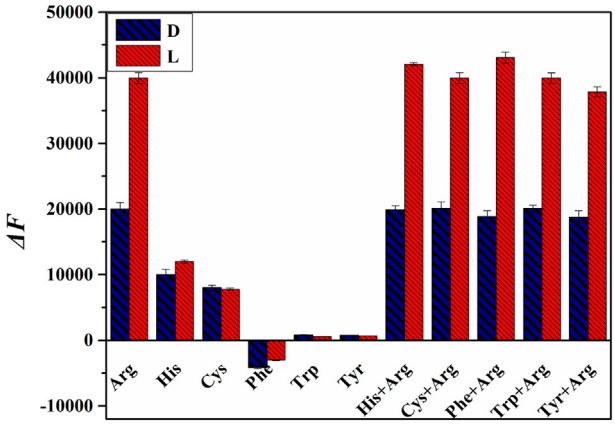

Fig. 14. Selectivity of the assay. The fluorescence enhancement of Aptamer + AuNps system in the presence of 50 nM D/L-Arg and 0.5 μM other amino acid (where red column represented D-amino acids and blue column represented L-amino acids). Experimental conditions: AuNps, 10 nM; Apt, 60 nM; pH = 7.2. (For interpretation of the references to color in this figure legend, the reader is referred to the web version of this article.)

3.6. Selectivity of the Proposed Aptamer-AuNps Fluorescence Chiral Bio-sensor for Arg Enantiomers

Under optimized conditions, other chiral amino acids enantiomers including His, Cys, Phe, Trp and Tyr were selected to study the selectivity. As displayed in Fig. 14, compared with Arg enantiomers, no obvious increase in fluorescence intensity was observed when respectively adding His, Cys, Phe, Trp, Tyr into aptamer + AuNps system. In contrast, when adding Arg enantiomers into the above non-Arg system again, the fluorescence intensity increased again. These results confirmed that this proposed new fluorescence method based on aptamer-AuNps biosensor has desirable selectivity for Arg enantiomers.

4. Real Sample Assay

In order to evaluate the practicality of the proposed method, the concentrations of L-Arg in urine samples were tested. When introducing the as-prepared urine samples into aptamer + AuNps system, the fluorescence intensity didn't enhanced, indicating there were no obvious matrix interference in urine samples, and then spiked certain amounts L-Arg into the above mentioned urine samples, the fluorescence intensity enhanced. As summarized in Table 2, the recovery of the spiked samples ranged from 97.5% to 107% implying that our method has the potential applicability for L-Arg determination in real samples.

5. Logic Operation

Molecular logic gates are widely established based on molecular recognition and assembly, and are promising to overcome the limitations of classical semiconductor devices [42,43]. Consequently, based on the aggregation of AuNps in the presence and absence of chiral Arg enantiomers, the "OR" logic gate was constructed with chiral Arg enantiomers (D,L-Arg) as inputs (Fig. 15). The absence and presence of inputs were

Table 2
Determination of L-Arg in human urine samples, for n = 5. Here, n stands for the number of replicates.

Number	Found (uM)	Added (uM)	Measured (uM)	Recovery (%)	RSD (%)
1	ND[a]	0	0		
2	ND[a]	0.1	0.103	103	0.9
3	ND[a]	0.2	0.195	97.5	1.5
4	ND[a]	0.3	0.327	107	1.2

[a] ND: not detected.

A

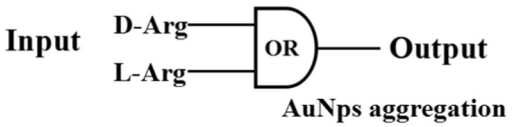

B

Input		Output
D-Arg	L-Arg	AuNPs aggregation
0	0	0
0	1	1
1	0	1
1	1	1

Fig. 15. Logic scheme of the "OR" logic gate A and truth B.

defined as "0" and "1". And the outputs of AuNps in aggregated and non-aggregated states were defined as "1" and "0", respectively. As mentioned above, the AuNps were dispersed after introducing into the Aptamers solutions, in contrast, when adding D-Arg or L-Arg into the above system, both AuNps based system were aggregated (in different degree). So a simple "OR" logic gate can be fabricated with D-Arg and L-Arg as inputs, and AuNps aggregation state as outputs. Only under the condition of no inputs (0,0), its output was "0". Under other conditions (0,1),(1,0) and (1,1), all the outputs were "1". That is to say, as long as one of the inputs exists, the logic gate (output) can be activated [44].

6. Conclusions

In summary, the FAM labeled aptamer was played as the fluorescence donor and the AuNps were played as the fluorescence receptor in this work. Together with aptamer and AuNps, the aptamer + AuNps bio-sensor was established to chiral recognition of Arg enantiomers. This fluorescence method exhibited a lower detection limit and a relatively wider linear rang compared with other Arg detection methods. What's more, this method was successfully applied in real sample detection with satisfactory results. Furthermore, the sensing system enable the design of an "OR" logic gate. All these above advantages indicated this method is promising in real-time testing for applicable purpose and could be applied in clinical diagnostics.

Supplementary data to this article can be found online at https://doi.org/10.1016/j.saa.2018.04.038.

Acknowledgements

This work was financially supported by the National Natural Science Foundation of China (21175015 and 21475014), and all authors here express their deep gratitude.

References

[1] W. Lenz, R.A. Pfeiffer, W. Kosenow, D.J. Hayman, Lancet 279 (1962) 45–46.
[2] Neelam Verma, Ashish Kumar Singh, Minni Singh, Biochemistry and Biophysics Reports, 12, 2017 228–239.
[3] Z.A. Carter, R. Kataky, Sensors Actuators B Chem. 243 (2017) 904–909.
[4] P.J. Andrew, B. Mayer, Cardiovasc. Res. 43 (1999) 521–531.
[5] M.M. Song, Z.Y. Sun, C.P. Han, D.M. Tian, H.B. Li, L. Jiang, Chem. Eur. J. 20 (2014) 1–8.
[6] J.J. Ou, L. Kong, C.S. Pan, X.Y. Su, X.Y. Lei, H.F. Zou, J. Chromatogr. A 2 (2006) 163–169.
[7] P. Sun, K. Arthi, Y. Abishek, S. Shreeyukta, M.M. Frederick, W.A. Daniel, Inorg. Chem. 46 (2007) 10312–10320.
[8] J.S. Jeon, H.T. Kim, Int. J. Cosmet. Sci. 38 (2016) 286–293.
[9] J.I. Langridge, T.D. McClure, S. El-Shakawi, A. Fielding, K.H. Schram, R.P. Newton, Rapid Commun. Mass Spectrom. 7 (1993) 427–434.
[10] Mufarreh Asmari, Lenka Michalcová, Sami El Deeb, et al., Microchem. J. 137 (2018) 98–104.
[11] Zhenzhen Lin, Shuzhen Lv, Kangyao Zhang, Dianping Tang, J. Mater. Chem. B 5 (2017) 826–833.
[12] Z. Qiu, J. Shu, D. Tang, Anal. Chem. 89 (2017) 5152.
[13] F. Shahdost-fard, A. Salimi, S. Khezrian, Biosens. Bioelectron. 53 (2014) 355–362.
[14] J.L. Steven, A.K. Elizabeth, A.S. Jay, Langmuir 22 (2006) 10535–10539.
[15] Z. Gao, N. Liu, Q. Cao, L. Zhang, S. Wang, W. Yao, F. Chao, Biosens. Bioelectron. 24 (2009) 1445–1450.
[16] C. Tuerk, L. Gold, Science 249 (1990) 505–510.
[17] A.D. Ellington, J.W. Szostak, Nature 346 (1990) 818–822.
[18] C. Tuerk, L. Gold, Science 249 (1990) 505–510.
[19] B. Prieto-Simón, M. Campàs, J.L. Marty, Bioanal. Rev. 1 (2010) 141–157.
[20] Baozhu Zhang, Chunying Wei, RSC Adv. 7 (2017) 56289–56295.
[21] M. Roushani, F. Shahdost-Fard, Anal. Chim. Acta 853 (2015) 214–221.
[22] Kangyao Zhang, Shuzhen Lv, Zhenzhen Lin, Meijin Li, Dianping Tang, Biosens. Bioelectron. 101 (2018) 159–166.
[23] Zhenli Qiu, Jian Shu, Dianping Tang, Anal. Chem. 90 (1) (2018) 1021–1028.
[24] Qian Zhou, Youxiu Lin, Kangyao Zhang, Meijin Li, Dianping Tang, Biosens. Bioelectron. 101 (2018) 146–152.
[25] S. Song, L. Wang, J. Li, C. Fan, J. Zhao, Trends Anal. Chem. 27 (2008) 108–117.
[26] Yuan Huo, Liang Qi, Xiao-Jun Lv, Ting Lai, Jing Zhang, et al., Biosens. Bioelectron. 78 (2016) 315–320.
[27] Xin Lv, Yuanfu Zhang, Guofu Liu, Du Lingyun, Shuhao Wang, RSC Adv. 7 (2017) 16290–16294.
[28] Yuan Huo, Liang Qi, Xiaojun Lv, Ting Lai, Jing Zhang, Zhi-Qi Zhang, Biosens. Bioelectron. 78 (2016) 315–320.
[29] Pengjuan Wang, Ying Wan, Aldalbahi Ali, Shengyuan Deng, Su Yan, Chuanhai Fan, Shulin Yang, Sci. Chin. Chem. 2 (2016) 237–242.
[30] Xin Lv, Yuanfu Zhang, Guofu Liu, Du Lingyun, Shuhao Wang, RSC Adv. 7 (2017) 16290–16294.
[31] Jiangtao Ren, Jiahai Wang, Jin Wang, Nathan W. Luedtked, Erkang Wang, Biosens. Bioelectron. 35 (2015) 401–406.
[32] R. Stoltenburg, C. Reinemann, B. Strehlitz, Anal. Bioanal. Chem. 383 (2005) 83–91.
[33] S. Zhan, Y. Wu, L. Wang, X. Zhan, P. Zhou, Biosens. Bioelectron. 86 (2016) 353–368.
[34] Zhen Zhang, Meng Zhang, Yong-Ill Lee, et al., Microchem. J. 124 (2016) 181–187.
[35] Yu-Feng Zhu, Yong-Sheng Wang, Xiao-Feng Wang, et al., Anal. Bioanal. Chem. 409 (2017) 4951–4958.
[36] R. Stoltenburg, C. Reinemann, B. Strehlitz, Anal. Bioanal. Chem. 383 (2005) 83–91.
[37] M. Roushani, F. Shahdost-Fard, Anal. Chim. Acta 853 (2015) 214–221.
[38] M.M. Maye, L. Han, N.N. Kariuki, N.K. Ly, W.-B. Chan, J. Luo, C.-J. Zhong, Anal. Chim. Acta. 496 (2003) 17–27.
[39] K.C. Grabar, R.G. Freeman, M.B. Hommer, M.J. Natan, Anal. Chem. 67 (1995) 735–743.
[40] Y. Wu, S. Zhan, F. Wang, L. He, W. Zhi, P. Zhou, Chem. Commun. 48 (2012) 4459–4461.
[41] S. Zhan, Y. Wu, L. Wang, X. Zhan, P. Zhou, Biosens. Bioelectron. 86 (2016) 353–368.
[42] Lu Wenjing, Yifang Gao, Yuan Jiao, Shaomin Shuang, Chenzhong Li, Chuan Dong, Nano 9 (2017) 11545–11552.
[43] Yusheng Yuan, Shaopu Liu, Xiaoli Hu, et al., Sensors Actuators B Chem. 236 (2016) 565–573.
[44] Jiangtao Ren, Jiahai Wang, Erkang Wang, Chem. Commun. 19 (2013) 479–483.